Paradoxical Enhancement of the Power Factor of Polycrystalline Silicon as a Result of the Formation of Nanovoids

B. Lorenzi, D. Narducci, R. Tonini, S. Frabboni, G. C. Gazzadi, G. Ottaviani, N. Neophytou & X. Zianni

Journal of Electronic Materials

ISSN 0361-5235
Volume 43
Number 10

Journal of Elec Materi (2014)
43:3812-3816
DOI 10.1007/s11664-014-3170-x

Springer

Journal of ELECTRONIC MATERIALS, Vol. 43, No. 10, 2014
DOI: 10.1007/s11664-014-3170-x

Paradoxical Enhancement of the Power Factor of Polycrystalline Silicon as a Result of the Formation of Nanovoids

B. LORENZI,[1,8] D. NARDUCCI,[1,9] R. TONINI,[2,10] S. FRABBONI,[2,3,11] G.C. GAZZADI,[3,12] G. OTTAVIANI,[2,13] N. NEOPHYTOU,[4,5,14] and X. ZIANNI[6,7,15]

1.—Department of Materials Science, University of Milano Bicocca, Milan, Italy. 2.—Department of FIM, University of Modena and Reggio Emilia, Modena, Italy. 3.—CNR, Institute of Nanoscience-S3, Modena, Italy. 4.—Institute for Microelectronics, Technical University of Vienna, Vienna, Austria. 5.—School of Engineering, University of Warwick, Coventry, UK. 6.—Department of Aircraft Technology, Educational Institution of Sterea Ellada, Psachna, Greece. 7.—Department of Microelectronics, IAMPPNM, NCSR Demokritos, Athens, Greece. 8.—e-mail: b.lorenzi2@campus.unimib.it. 9.—e-mail: dario.narducci@unimib.it. 10.—e-mail: rita.tonini@unimore.it. 11.—e-mail: stefano.frabboni@unimore.it. 12.—e-mail: giancarlo.gazzadi@unimore.it. 13.—e-mail: giampiero.ottaviani@unimore.it. 14.—e-mail: neophytou@iue.tuwien.ac.at. 15.—e-mail: xzianni@gmail.com

Hole-containing silicon has been regarded as a viable candidate thermoelectric material because of its low thermal conductivity. However, because voids are efficient scattering centers not just for phonons but also for charge carriers, achievable power factors (PFs) are normally too low for its most common form, i.e. porous silicon, to be of practical interest. In this communication we report that high PFs can, indeed, be achieved with nanoporous structures obtained from highly doped silicon. High PFs, up to a huge 22 mW K^{-2} m^{-1} (more than six times higher than values for the bulk material), were observed for heavily boron-doped nanocrystalline silicon films in which nanovoids (NVs) were generated by He^+ ion implantation. In contrast with single-crystalline silicon in which He^+ implantation leads to large voids, in polycrystalline films implantation followed by annealing at 1000°C results in homogeneous distribution of NVs with final diameters of approximately 2 nm and densities of the order of 10^{19} cm^{-3} with average spacing of 10 nm. Study of its morphology revealed silicon nanograins 50 nm in diameter coated with 5-nm precipitates of SiB_x. We recently reported that PFs up to 15 mW K^{-2} m^{-1} could be achieved for silicon–boron nanocomposites (without NVs) because of a simultaneous increase of electrical conductivity and Seebeck coefficient. In that case, the high Seebeck coefficient was achieved as a result of potential barriers on the grain boundaries, and high electrical conductivity was achieved as a result of extremely high levels of doping. The additional increase in the PF observed in the presence of NVs (which also include SiB_x precipitates) might have several possible explanations; these are currently under investigation. Experimental results are reported which might clarify the reason for this paradoxical effect of NVs on silicon PF.

Key words: Silicon, thermoelectricity, nanovoids, energy filtering

INTRODUCTION

Despite its low thermoelectric (TE) efficiency, it would be highly desirable to use silicon as a material for TE conversion because of the large scientific and technological know-how available for silicon, and because of the easy integration of Si-based TE devices. As is well known, the low TE efficiency of silicon is because of its high thermal conductivity (ranging from ≈130 W K^{-1} m^{-1} in intrinsic single-crystal silicon[1] to ≈25 W K^{-1} m^{-1} in nanocrystalline

(Received October 25, 2013; accepted April 5, 2014; published online May 6, 2014)

silicon[2]) and to its relatively low power factor (PF) ($\leq$3 mW K^{-2} m^{-1}—although larger values, up to 6.3 mW K^{-2} m^{-1} at 350 K, have recently been reported[3]). In previous papers[4–6] we have reported that, upon boron precipitation, PFs as high as 15 mW K^{-2} m^{-1} can be achieved for highly boron-doped nanocrystalline silicon at 300 K. To reduce its thermal conductivity, introduction of voids by He^+-implantation seems a viable technique, possibly with marginal reduction of hole conductivity. Previous literature[7,8] reported contrasting results, clearly suggesting an effect of pore size and structure on both PF and thermal conductivity.

The purpose of this paper is to report preliminary results obtained from thermoelectric characterization of heavily doped nanocrystalline silicon implanted with He^+. It is shown that He^+ implantation followed by annealing leads to the formation of nanovoids that, rather unexpectedly, improve the PF of the material. Although the data currently available are, admittedly, incomplete, they are consistent with models and results previously reported for heavily doped nanocrystalline silicon and may be expected to increase the interest of the thermoelectric community because of the exceptionally high PF.

EXPERIMENTAL

Polycrystalline silicon films 450 nm thick were deposited by chemical vapor deposition (CVD) on to oxidized single-crystal silicon substrates. Films were doped with boron by ion implantation (60 keV, 2×10^{16} cm^{-2}) to a nominal total boron concentration of 4.4×10^{20} cm^{-3} and submitted to standard damage-recovery treatment (1050°C, 30 s in N_2). An 250 nm thick sacrificial aluminium layer was then deposited by sputtering on to the films, and the films were then implanted with helium in a two-step process (90 keV, 4×10^{16} cm^{-2} + 58 keV, 1.5×10^{16} cm^{-2}). To prevent contamination and to match the 90 keV He end-of-range distribution within the poly layer, the aluminium layer was then removed by etching in HCl. Finally, a standard cleaning treatment (piranha etch, 90°C, 30 min, followed by 3% mol. HF) was conducted before evaporating Al–Si 1% electrical contacts through a shadow mask. Thermal desorption spectra obtained at constant heating rate revealed behavior similar to that of the single crystal[9] with He fully desorbing at 800°C.

Samples were submitted to annealing in argon to analyze the structural and functional evolution of the films. Metal contacts were removed by HCl etching before each annealing and redeposited afterward.

Samples for Seebeck coefficient and the electrical conductivity measurements were 50 mm^2 × 50 mm^2 rectangular chips; Hall measurements were performed on 17 mm^2 × 17 mm^2 samples with aluminium contacts evaporated on small areas in the four corners, in accordance with Van der Pauw geometry. Hall measurements were performed at room temperature (298 K) using a maximum magnetic field of 0.5 T. Accuracy was found to be better than ±1%. Precision was estimated, on the basis of the deviation of contact design relative to the ideal Van der Pauw configuration,[10] to be +0/−17% for Hall mobility and +18/−0% for carrier density p. Seebeck coefficient and electrical conductivity were measured by use of a home-built system. For Seebeck coefficient measurements the integral method[11] was used, fixing the temperature of the cold contact at 20°C while heating the other contact between 40°C and 120°C. Conductivity was determined from current–voltage characteristics at 20°C. Each set of Seebeck coefficient measurements was repeated on the same sample at least three times to ensure data reliability. Also, charge-transport coefficients were measured on nominally identical samples and found to be reproducible within ±10%. The whole experimental setup was calibrated by use of single-crystal silicon samples of known doping level.

Cross-sections for electron microscopy (EM) were prepared by both conventional and focused-ion beam lift-out methods. EM analysis was performed both by low-energy (30 keV) dark-field scanning transmission EM (DF-STEM) and by high-energy (200 keV) transmission (TEM). Low-energy analysis was performed with a bright field (BF)–dark field (DF) solid state detector. TEM and energy-filtered electron spectroscopic images (ESI) were obtained by use of an electron microscope with spherical aberration coefficient 0.5 mm, chromatic aberration coefficient 1.1 mm, and equipped with conventional LaB_6 electron source and an electron energy loss imaging filter. This attachment enables recording of both electron energy loss spectroscopy (EELS) data and ESI.

To evaluate the density of helium atoms effectively present inside the silicon lattice, temperature programmed desorption (TPD) measurements were performed after helium implantation. TPD experiments, consisting in measurement of helium effusion rate during thermal treatment in a temperature ramp with assigned heating rate, is an ideal technique to study the evolution toward stable cavities of vacancy-like defects in helium-implanted silicon. It can actually give information about the kinds and states of the structures in which helium is trapped. TPD spectra were performed at a pressure of $\approx 10^{-6}$ mbar, with a ramp of 0.75°C/s in the temperature range 80–800°C.

RESULTS

Heat treatment promotes three simultaneous diffusion processes:

1. vacancy diffusion, leading to the final formation of nanovoids;

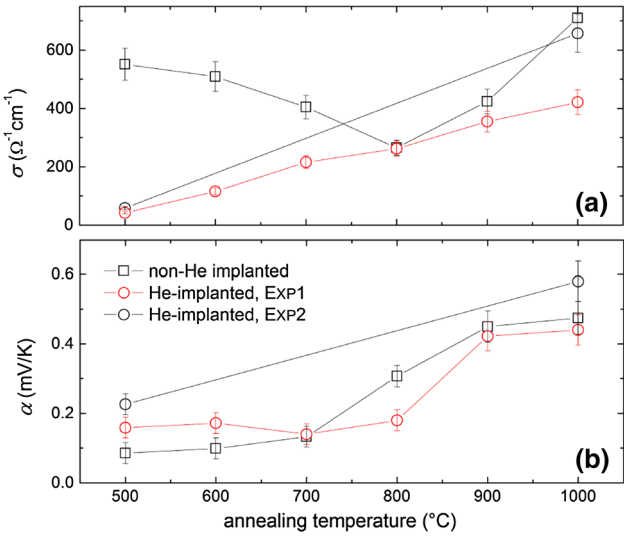

Fig. 1. (a) Electrical conductivity and (b) Seebeck coefficient vs. annealing temperature on sequential annealing in Ar from 500°C to 1000°C in 2-h long, 100° steps (Exp1) and upon two-hour annealing at 500°C and 1000°C only (Exp2) compared with non-He implanted samples annealed in Ar from 500°C to 1000°C in 2-h long, 100° steps.

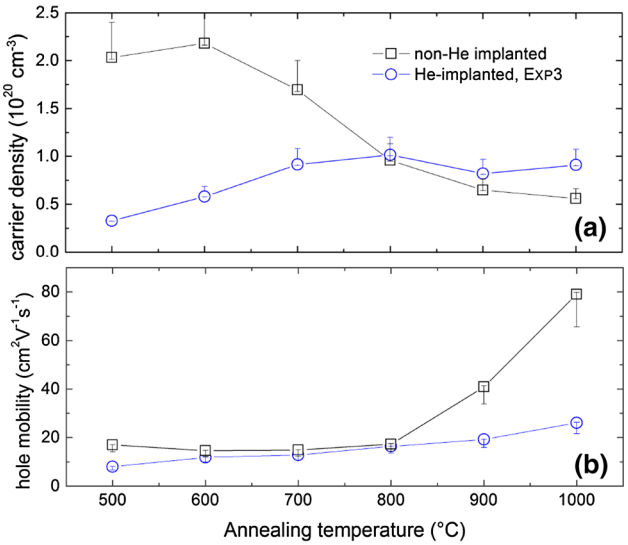

Fig. 2. (a) Carrier density and (b) hole mobility vs. annealing temperature on sequential annealing in Ar from 500 to 1000°C in 30-min long, 100° steps (Exp3).

2. boron diffusion, resulting in its segregation at grain boundaries (GBs) and then, eventually, to its precipitation as a second phase; and
3. helium outdiffusion from silicon.

Because the three processes are characterized by different rates, several sets of sequential annealing cycles were performed. In the first, we analyzed the variations of σ and α upon annealing for 2 h in steps of 100°from 500°C to 1000°C. In the second, a shorter cycle was implemented, the samples being sequentially annealed for 2 h at 500°C and 1000°C only. We will refer to these two experiments as Exp1 and Exp2, respectively.

The evolution of the Seebeck coefficient α in Exp1 followed a trend closely reminiscent of that observed for non-He-implanted (nHeI) samples[4,6] (Fig. 1). The Seebeck coefficient increased rather abruptly on annealing at 800°C, reaching a maximum value of 0.45 mV/K after annealing at 1000°C. In contrast, the electrical conductivity σ increased almost linearly with annealing temperature T_a, quite different from that observed for nHeI specimens.

It is interesting to compare such a trend with that observed in Exp2. Whereas both σ and α after annealing at 500°C are similar in the two experiments, Exp2 leads to an electrical conductivity at 1000°C closely comparable to that of the nHeI samples whereas Exp1 results in a final σ value approximately half that observed in the absence of helium implantation. In contrast, the final Seebeck coefficient in Exp1 was equal to that for the nHeI material whereas in Exp2 the final α value is approximately 15% larger.

To clarify these differences, Hall effect measurements were conducted. We performed the sequential annealing under conditions intermediate between Exp1 and Exp2—namely 30-min annealing from 500°C to 1000°C in 100°steps (Fig. 2). We will refer to this annealing cycle as Exp3. As expected, the steady increase of σ observed for all He-implanted samples is apparently caused by the regular increase of the hole mobility μ, changing by almost a factor of four from the as-implanted to the fully cured film.

With regard to carrier density, for nHeI specimens p reflected the diffusion-limited precipitation of boron from the supersaturated Si-B solid solution.[4,5] A different $p(T_a)$ trend is observed in Exp3, in which p increased smoothly by a factor of five on annealing up to 700°C, then leveling to 10^{20} cm^{-3}—a value close to that measured for nHeI films—at higher annealing temperatures.

TPD analysis performed on as-implanted samples revealed a total effusive helium fluence of 4.5×10^{16} cm^{-2}. These results are compatible with those reported in the literature for single-crystalline samples,[12] showing the amounts of helium implanted and outdiffusing were no different from those for polycrystalline samples. A single outdiffusion peek was found at 780°C.

TEM provided information about the formation of voids and precipitates. Helium implantation in single-crystal silicon has been the subject of several investigations in recent years.[12–14] In summary, radiation damage is known to generate a large excess of vacancies (and other defects) in the crystal. On annealing at temperatures above 300°C, vacancies begin to cluster, leading to the formation of He-filled platelets, when then evolve to form voids. In parallel, helium outdiffuses with three desorption peaks at 450–500°C, 650°C, and 800°C,[9] because its solution enthalpy in silicon is positive

(0.84 eV). Annealing at temperatures higher than 600°C promotes enlargement of voids and their reshaping to reach their minimum free energy shape (approximately that of a tetrakaidecahedron). We will refer to this type of object as *mesovoids*.

Much less is known about the evolution of He-generated vacancies in polysilicon, although it is obviously dependent on the pristine micromorphology of the material.[15,16] In this work, TEM images of polysilicon films before He implantation (Fig. 3a) are indicative of approximately bimodal in-depth distribution of grain size, with a top layer, approximately 200-nm thick, characterized by larger lateral grain sizes of approximately 80 nm; and an inner layer with smaller grains (lateral grain size ≈50 nm) extending for another 250 nm. DF-STEM images of films annealed at 1000°C for 2 h in argon reveal no significant modification of grain size or shape (Fig. 3b). Although possibly surprising, this observation is in good agreement with previous accounts for heavily boron doped polycrystalline silicon, for which marginal (if any) grain size variations at temperatures as high as 900°C were reported.[17] Also, as reported in previous publications,[18] TEM bright field images (Fig. 3c) show diffraction contrast details, particularly at GBs, strongly suggesting the formation of boron-rich precipitates (SiB_x).

Samples implanted with He were comparatively analyzed by TEM at the end of each step of Exp2 (Fig. 3d, e). Although film morphology was similar to that observed for nHeI—nanograins ≈50 nm in diameter coated by 5-nm SiB_x precipitates—we observed homogeneous distribution of *nanovoids* with diameters of approximately 5 nm at 500°C, either disappearing or shrinking to subnanometer sizes at 1000°C. Also, mesovoids of irregular shape are observed at GBs. Further analysis of void dynamics in nanocrystalline silicon is reported in a companion paper presented at this conference.[19]

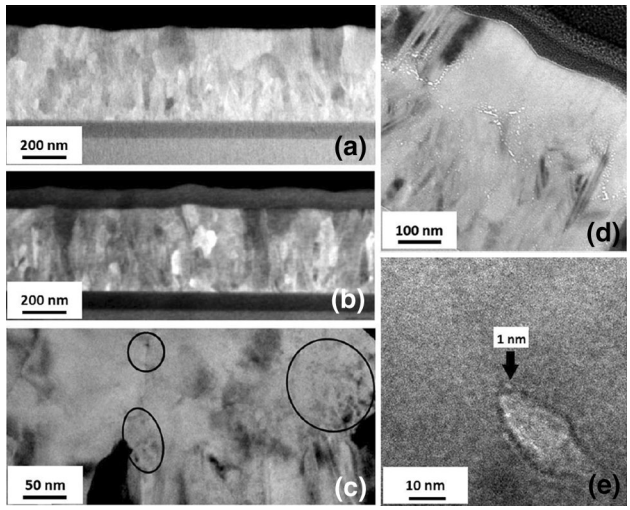

Fig. 3. (a) DF-STEM image of the as-deposited non-He implanted sample; (b) DF-STEM and (c) TEM bright field image of the same sample after annealing at 1000°C. Circled areas in the TEM image mark diffraction contrast details relating to SiB_x precipitates. Note also the preservation of grain sizes on annealing at high temperature. (d) TEM images of the He-implanted sample upon annealing at 500°C for 2 h and (e) upon subsequent annealing at 1000°C for 2 h. Note the distribution of nanovoids throughout the grains, their size shrinking to sub-nanometer size when the annealing temperature is increased.

DISCUSSION

This preliminary evidence confirms that film properties are controlled by the simultaneous occurrence of vacancy and helium diffusion, and of boron diffusion-limited precipitation, leading to the generation of nanovoids and to the formation of an SiB_x second phase.

In the longest processing sequence (Exp1), variation of the Seebeck coefficient basically reproduces that observed in nHeI specimens submitted to the same annealing sequence. The concurrent increase of σ and α with annealing temperature is in good agreement with the theory of carrier energy filtering in two-phase systems.[20,21] The conductivity is however smaller than in nHeI samples as a combined effect of the damage recovery (at low T_a) and of the residual presence of shrunk nanovoids (at high T_a).

On lowering the duration of the annealing sequence (Exp3) one observes how initially different values of carrier densities in implanted and non-implanted films tend to very similar values for $T_a \geq 800$°C. The concentration of dissolved (electrically active) boron differs substantially on He implantation, because most of the boron is deactivated by implantation damage. Annealing enables recovery. Also, because it is known that the decrease of carrier density in nHeI samples at high annealing temperatures is because of partial precipitation of boron to form SiB_x precipitates, the likely evolution of $p(T_a)$ in nHeI and Exp3 samples suggests that precipitation also occurs in Exp3 specimens. This also explains the increase of hole mobility at $T_a \geq 800$°C, that is accounted for once again by the occurrence of energy filtering in the presence of precipitates. As in Exp1, however, one expects μ values lower than those found in nHeI samples, because of incomplete damage recovery in the low T_a range and because of the residual presence of nanovoids at higher T_a.

Finally, the shortest annealing cycle (Exp2) apparently leads to an increase of α above that observed for nHeI films, indicative of an effect of sub-nanometric voids. Hall measurements are currently in progress. In the absence of carrier density data it may, anyway, be conjectured that in the depletion region surrounding NVs a lower carrier density (and, as a result, a larger fraction of neutral dopants) would be found. Alternative mechanisms reducing hole density might be related to the large concentration of vacancies made available by the (partially) dissolved voids, thus favoring the formation of boron-vacancy ($B_S V_2$) complexes

that would shift the acceptor level deeper into the energy gap.[22] In both cases the lower carrier density would lead to a larger Seebeck coefficient. Also, because ionized impurity-limited mobility linearly depends on the reciprocal of carrier density,[23] reduction of p would be compensated by an increase of μ, thus justifying a conductivity comparable with that observed in nHeI films.

Although no detailed analysis of stability was conducted, on the basis of the results for single-crystalline silicon one may argue that polycrystalline He-implanted films also should be stable up to 800°C. Actually, between 500°C and 800°C all active processes involving voids are driven by the differential pressure of He in differently sized He-filled voids. Because helium has already left the voids in samples annealed up to 1000°C, no driving force is expected that might cause micromorphological modification of the material. Thus, one may expect this type of system to be of interest for relatively high-temperature applications also.[24]

CONCLUSIONS

In this paper we have reported preliminary results from thermoelectric characterization of heavily doped nanocrystalline silicon implanted with He^+. It has been shown that He^+ implantation followed by annealing leads to the formation of nanovoids. Their dynamics were found to differ substantially from those observed for monocrystalline silicon, with much tinier voids forming at 500°C that further shrink at higher annealing temperatures. Also, thermal processing was found to either not affect or further enhance silicon PF, leading to a record value of 22 mW K^{-2} m^{-1}. The results could be qualitatively explained on the basis of a previously proposed energy-filtering model. Thermal conductivity measurement is currently in progress and complete data for this very promising Si-based system will be reported in forthcoming papers.

REFERENCES

1. J.A. Carruthers, T.H. Geballe, H.M. Rosenberg, J.M. Ziman, *Proc. R. Soc.* 238, 502 (1957).
2. Y.C. Tai, C.H. Mastrangelo, R.S. Muller, *J. Appl. Phys.* 63(5), 1442 (1988).
3. A. Stranz, J. Khler, A. Waag, E. Peiner, *J. Electron. Mater.* 42(7), 2381 (2013).
4. D. Narducci, E. Selezneva, A. Arcari, G. Cerofolini, E. Romano, R. Tonini, and G. Ottaviani, in *MRS Online Proc. Library*, Vol. 1314 (MRS, 2011), Mrsf10-1314-ll05-16.
5. D. Narducci, E. Selezneva, G. Cerofolini, S. Frabboni, G. Ottaviani, *AIP Conf. Proc.* 1449(1), 311 (2012).
6. D. Narducci, E. Selezneva, G. Cerofolini, S. Frabboni, G. Ottaviani, *J. Solid State Chem.* 193, 19 (2012).
7. J. Tang, H.T. Wang, D.H. Lee, M. Fardy, Z. Huo, T.P. Russell, P. Yang, *Nano Lett.* 10(10), 4279 (2010).
8. J. Boor, D. Kim, X. Ao, M. Becker, N. Hinsche, I. Mertig, P. Zahn, V. Schmidt, *Appl. Phys. A* 107(4), 789 (2012).
9. G.F. Cerofolini, G. Calzolari, F. Corni, S. Frabboni, C. Nobili, G. Ottaviani, R. Tonini, *Phys. Rev. B* 61, 10183 (2000).
10. L.J. Van Der Pauw, *Philips Res. Rep.* 13(1), 1 (1958).
11. C. Wood, A. Chmielewski, D. Zoltan, *Rev. Sci. Instrum.* 59(6), 951 (1988).
12. S. Frabboni, F. Corni, C. Nobili, R. Tonini, G. Ottaviani, *Phys. Rev. B* 69, 165209 (2004).
13. E. Romano, G.F. Cerofolini, D. Narducci, F. Corni, S. Frabboni, G. Ottaviani, R. Tonini, *Surf. Sci.* 603(14), 2188 (2009).
14. V. Raineri, M. Saggio, E. Rimini, *J. Mater. Res.* 15(7), 1449 (2000).
15. W. Beyer, R. Carius, U. Zastrow, *J. Non-Cryst Solids* 352(9–20), 1402 (2006).
16. K.J. Abrams, S.E. Donnelly, M.F. Beaufort, J. Terry, L.I. Haworth, D. Alquier, *Phys. Status Solidi C* 6(8), 1964 (2009).
17. H.J. Kim and C.V. Thompson, *MRS Proceedings*, Vol. 106, p. 143.
18. D. Narducci, E. Selezneva, G. Cerofolini, E. Romano, R. Tonini, G. Ottaviani, *Proceedings of the 8th European Conference on Thermoelectric* (CNR, Como, 2010), p. 141.
19. B. Lorenzi, S. Frabboni, G. Gazzadi, R. Tonini, G. Ottaviani, and D. Narducci, *J. Electron. Mater.* In press (2014).
20. N. Neophytou, X. Zianni, M. Ferri, A. Roncaglia, G. Cerofolini, D. Narducci, *J. Electron. Mater.* 42, 2393 (2013).
21. N. Neophytou, X. Zianni, H. Kosina, S. Frabboni, B. Lorenzi, D. Narducci, *Nanotechnology* 24(20), 205402 (2013).
22. J. Adey, R. Jones, D.W. Palmer, P.R. Briddon, S. Öberg, *Phys. Rev. B* 71, 165211 (2005).
23. D. Chattopadhyay, H.J. Queisser, *Rev. Mod. Phys.* 53(4), 745 (1981).
24. S. Kumar, S. Heister, X. Xu, J. Salvador, G. Meisner, *J. Electron. Mater.* 42(4), 665 (2013).